2008

Receptor-binding, biodistribution, and metabolism studies of 64Cu-DOTA-cetuximab, a PET-imaging agent for epidermal growth-factor receptor-positive tumors

Wen Ping Li
Washington University School of Medicine in St. Louis

Laura A. Meyer
Washington University School of Medicine in St. Louis

David A. Capretto
Washington University School of Medicine in St. Louis

Christopher D. Sherman
Washington University School of Medicine in St. Louis

Carolyn J. Anderson
Washington University School of Medicine in St. Louis

CANCER BIOTHERAPY & RADIOPHARMACEUTICALS
Volume 23, Number 2, 2008

DOI: 10.1089/cbr.2007.0444

Receptor-Binding, Biodistribution, and Metabolism Studies of ^{64}Cu-DOTA-Cetuximab, a PET-Imaging Agent for Epidermal Growth-Factor Receptor-Positive Tumors

Wen Ping Li, Laura A. Meyer, David A. Capretto, Christopher D. Sherman, and Carolyn J. Anderson
Mallinckrodt Institute of Radiology, Washington University School of Medicine, St. Louis, MO

ABSTRACT

The epidermal growth-factor receptor (EGFR) and its ligands have been recognized as critical factors in the pathophysiology of tumorigenesis. Overexpression of the EGFR plays a significant role in the tumor progression of a wide variety of solid human cancers. Therefore, the EGFR represents an attractive target for the design of novel diagnostic and therapeutic agents for cancer. Cetuximab (C225, Erbitux®) was the first monoclonal antibody targeted against the ligand-binding site of EGFR approved by the Food and Drug Administration for the treatment of patients with EGFR-expressing, metastatic colorectal carcinoma, although clinical trials showed variability in the response to this treatment. The aim of this study involved using cetuximab to design a positron emission tomography (PET) agent to image the overexpression of EGFR in tumors. Cetuximab was conjugated with the chelator, DOTA, for radiolabeling with the positron-emitter, ^{64}Cu ($T_{1/2}$ = 12.7 hours). ^{64}Cu-DOTA-cetuximab showed high binding affinity to EGFR-positive A431 cells (K_D of 0.28 nM). Both biodistribution and microPET imaging studies with ^{64}Cu-DOTA-cetuximab demonstrated greater uptake at 24 hours postinjection in EGFR-positive A431 tumors (18.49% ± 6.50% injected dose per gram [ID/g]), compared to EGFR-negative MDA-MB-435 tumors (2.60% ± 0.35% ID/g). A431 tumor uptake at 24 hours was blocked with unlabeled cetuximab (10.69% ± 2.72% ID/g), suggesting that the tumor uptake was receptor mediated. Metabolism experiments in vivo *showed that ^{64}Cu-DOTA-cetuximab was relatively stable in the blood of tumor-bearing mice; however, there was significant metabolism in the liver and tumors. ^{64}Cu-DOTA-cetuximab is a potential agent for imaging EGFR-positive tumors in humans.*

Key words: epidermal growth-factor receptor, PET imaging, copper-64, monoclonal antibody

INTRODUCTION

Membrane receptors of the tyrosine kinase family are the best-characterized targets in cancer cells. The epidermal growth factor (EGF) family of membrane receptors is one of the most relevant targets in this class. Epidermal growth-factor receptor (EGFR) is associated with oncogenic transformation, and the dysregulation of EGFR is associated with all of the key features of cancer, such as autonomous cell growth, invasion, angiogenic potential, and the development of distant metastases.[1] An increased expression of EGFR is the hallmark of many human tumors, such as breast cancer, squamous-cell carcinoma

Address reprint requests to: Carolyn J. Anderson; Mallinckrodt Institute of Radiology, Washington University School of Medicine; 510 South Kingshighway Boulevard, Campus Box 8225, St. Louis, MO 63110; Tel.: (314) 362-8427; Fax: (314) 362-9940
E-mail: **andersoncj@wustl.edu**

of the head and neck, and prostate cancer. Activation of EGFR contributes to several other essential tumorigenic mechanisms, including tumor survival, invasion, angiogenesis, and metastatic spread. In many tumors, EGFR expression may act as a prognostic indicator, predicting poor survival and/or more advanced disease stage.[2]

Of several therapeutic approaches to target EGFR, monoclonal antibodies (mAbs), which block the binding of EGF to the extracellular ligand-binding domain of the receptor and small tyrosine kinase inhibitors, are the furthest along in clinical development. In addition, mAbs inhibiting EGFR were the first approach used in clinical studies to target the aberrant signaling of EGFR in malignant cells.[1] As knowledge concerning the molecular nature of antigens associated with tumors increased, antibodies that bind with high affinity and specificity to cancer cells were developed. Cetuximab (C225, Erbitux®) was the first mAb targeted against the ligand-binding site of EGFR approved by the Food and Drug Administration for the treatment of patients with EGFR-expressing, metastatic colorectal carcinoma, although clinical trials have revealed significant variability in the response to this agent.[3–5] Cetuximab binds competitively to the extracellular domain of EGFR with an affinity comparable to the natural ligand ($K_D = 1.0$ nM), inhibiting the binding of the activating ligand to the receptor.[6,7] Consequently, cetuximab binding inhibits the autophosphorylation of EGFR and induces its internalization and degradation. The effective use of this new therapeutic agent that targets EGFR will depend on the ability of physicians to detect and characterize EGFR-expression in lesions before and after the initiation of treatments. A radiopharmaceutical for noninvasively measuring tumor EGFR overexpression *in vivo* would provide important information on the expression levels of EGFR-targeting agents and potentially aid in the optimization of cancer treatment plans.

The use of radiolabeled anti-EGFR antibodies for EGFR-expressing cancer diagnosis has become the subject of intense investigation as more mAbs with relevant, well-characterized specificities become available. The ^{111}In-labeled anti-EGFR antibody, 425, successfully detected malignant gliomas, and the ^{99m}Tc-labeled anti-EGFR humanized antibody, hR3, is under clinical evaluation.[8,9] Cetuximab attached to the radiometal chelator, diethylenetriaminepentaacetic acid (DTPA), and labeled with ^{111}In, was shown to localize specifically in tumors that overexpress EGFR.[10,11] However, a considerable amount of radioactivity in the liver was observed as a result of nonspecific uptake, thereby limiting the clinical usefulness of this agent for cancer imaging. An improved cetuximab conjugate (DTPA-PEG-cetuximab) was reported to overcome this problem, as tumor imaging of ^{111}In-DTPA-PEG-cetuximab in nude mice showed significant reduction of radioactivity in the liver using a gamma camera.[11] Although cetuximab Fab′ and $F(ab')_2$ fragments have been investigated, they have reduced binding affinity (5-fold weaker) and showed less inhibition of tumor growth than the intact antibody.[7] A smaller molecular weight "affibody," (Z(EGFR:955)),[2] that binds to EGFR, was labeled with ^{125}I, demonstrating that this technology holds promise for improving both targeting and nontarget organ clearance, compared to intact antibodies.[12]

The aim of this study involved using cetuximab to design a positron emission tomography (PET) imaging agent to image the overexpression of EGFR in tumors. PET has an advantage in terms of its greater sensitivity and higher resolution at all depths than a gamma camera or single-photon emission tomography (SPECT). Copper-64 (half-life, 12.7 hours; 17.4% β^+ [0.656 MeV]; 39% β^- [0.573 MeV]) is an attractive positron-emitting radionuclide for both PET imaging and radiotherapy and has a compatible half-life with the slow blood clearance of an antibody. Cai et al. recently reported the evaluation of ^{64}Cu-DOTA-cetuximab in several tumor-bearing mouse models.[13] In the present study, we also report on the development of ^{64}Cu-DOTA-cetuximab for the small-animal imaging of EGFR expression. Additionally, we report in this paper on the receptor binding of this radiopharmaceutical to EGFR, as well as the *in vivo* metabolism of ^{64}Cu-DOTA-cetuximab.

MATERIALS AND METHODS

1,4,7,10-tetraazacyclododecane-1,4,7-tris(t-butyl acetate)-10-acetic acid mono(N-hydroxysuccinimide ester) (DOTA-mono-NHS-tris(tBu) ester) was purchased from Macrocyclics (Dallas, TX). Centricon 100 concentrators were purchased from Amicon Inc. (Beverly, MA). Bio-Spin 6 chromatography columns were from Bio-Rad Laboratories (Hercules, CA). All chemicals used were purchased from Sigma-Aldrich Chemical Co. (St Louis, WI). All solutions were made by using distilled deionized water (Milli-Q, Mil-

lipore, Bedford, MA; ~18 MΩ resistivity). mAb cetuximab (C225) was kindly provided by ImClone Systems, Inc. (New York, NY). Eight (8) to 10-week-old female athymic nude mice were purchased from Charles River (Wilmington, MA). A Branson Sonifier (Branson, Danbury, CT) cell disrupter, a Tekmar (Tekmar, Malon, OH) tissue homogenizer, and a Sorvall (Thomas Scientific, Waltham, MA) RC2-B centrifuge were used in the cell binding and animal metabolism experiments. Size-exclusion high-performance liquid chromatography (HPLC), used in the conjugation and purification of radiolabeled conjugate, and in metabolite analyses, was accomplished on a Superose 12 HR 10/300 column (Amersham Biosciences, Uppsala, Sweden) with a Waters (Milford, MA) 2487 dual λ absorbance detector and an Ortec Model 661 (EG&G Instruments, Oak Ridge, TN) radioactive detector. The mobile phase was 20 mM HEPES and 150 mM NaCl [pH 7.3] eluted at a flow rate of 0.5 mL/min. Millenium 32 software (Waters) was used to quantify chromatograms by integration. A Beckman 8000 (Beckman, Fullerton, CA) automated well-typed gamma counter was used to count size-exclusion HPLC fractions of metabolite and animal biodistribution samples. Levels of radioactivity greater than 0.05 MBq were assayed in a Capintec dose calibrator (model-15R; Capintec, Ramsey, NJ). Multiscreen 96-well microtiter plates for receptor-binding assays were counted on a 1450 Microbeta Trilux Liquid Scintillation and Luminescence Counter (PerkinElmer Life Sciences, Downers Grove, IL). Copper-64 was produced, as previously reported, on a biomedical CS-15 cyclotron at the Washington University School of Medicine (St. Louis, MO).[14]

Conjugation of DOTA to Cetuximab and Radiolabeling with ^{64}Cu

DOTA was conjugated to cetuximab in 0.1 M of Na_2HPO_4 (pH 7.5), using an adaptation of the method described by Rogers et al.[15] Cetuximab (2 mg/mL) was washed with 0.1 M of Na_2HPO_4 (pH 7.5), using a Centricon 100 and then concentrated prior to conjugation with DOTA-mono-NHS-tris(tBu) ester. The volume of concentrated cetuximab was measured by pipetting and transferred into an acid-washed microcentrifuge tube. DOTA-mono-NHS-tris(tBu) ester was dissolved in 0.1 M of Na_2HPO_4 (pH 7.4) and the pH was adjusted to 7.4 by adding 0.1 M of NaOH. An aliquot of this solution was added to the concentrated cetuximab in a 90:1 molar ratio (DOTA-mono-NHS-tris(tBu)ester: cetuximab), followed by incubation at 4°C overnight with end-over-end rotation. The conjugate was then transferred to a Centricon 100, diluted to 2.0 mL with 0.1 M of ammonium citrate (pH 5.5), and centrifuged. This procedure was repeated four times to remove small-molecule reactants, and the conjugate was collected from the membrane. Purity and concentration of the resulting DOTA-cetuximab conjugate were determined by size-exclusion HPLC and stored at 4 °C until needed. Titration of DOTA-cetuximab with [^{nat}Cu]copper acetate spiked with ^{64}Cu revealed that the ratio of DOTA:cetuximab achieved by this procedure was 5.5.[16]

DOTA-cetuximab labeling with ^{64}Cu was carried out by adding DOTA-cetuximab to $^{64}CuCl_2$ in 0.1 M of ammonium citrate buffer [pH 5.5], followed by incubation for 1 hour at 40°C. The radiochemical purity of the resulting ^{64}Cu-DOTA-cetuximab was determined by size-exclusion HPLC, and purification was performed by using Bio-spin 6 or size-exclusion HPLC on a Superose 12 HR 10/300 column, if necessary. The specific activity ranged from 370 to 1110 MBq ^{64}Cu per milligram of cetuximab.

Cell Lines and Tumor Xenograft Mouse Models

Human vulvar squamous carcinoma A431 cells (high concentration of EGFR) were purchased from the American Type Culture Collection (ATCC; Manassas, VA) and maintained in Dulbecco's modified Eagle's medium (DMEM) containing 10% fetal bovine serum (FBS). Human breast adenocarcinoma MDA-MB-435 cells (low concentration of EGFR) were obtained from Janet E. Price, PhD (MD Anderson Cancer Center, Houston, TX)[17] and grown in DMEM supplemented with 10% FBS and antibiotics at 37°C and 5% CO_2. A431 cells have a high expression of EGFR, whereas MDA-MB-435 cells express low levels.[10] Female nu/nu mice (8–10 weeks of age) were injected subcutaneously with 5×10^6 A431 cells in the neck. Tumors reached appropriate size (0.3–0.5 g) on day 12, and all animal studies were performed at 12 days post-tumor implantation. The MDA-MB-435 human breast cancer model was established by injecting 4×10^5 cells/100 μL in the right mammary fat pad of 8–10-week-old female nu/nu mice, and the animal studies were carried out at 2 weeks post-tumor implantation.

In Vitro Binding Affinity

The receptor-binding properties of ^{64}Cu-DOTA-cetuximab were evaluated in direct radioligand competitive and saturation binding assays, using A431 and MDA-MB-435 cell lines.[10,18] Cell membranes were prepared by following the method described previously.[19] Briefly, cells were grown as a monolayer in 75 cm^2 tissue culture flasks (Falcon [BO Biosciences, San Jose, CA] or Costar) to about 90% confluence. The cells were gently washed with 3 mL of ice-cold 20 mM Tris-HCl (pH 7.4) before the addition of 5 mL of cold, freshly prepared homogenizing buffer (50 mM of Tris-HCl, pH 7.4, 5.0 mM of $MgCl_2$, 0.5 μg/mL of aprotinin, 200 μg/mL of bacitracin, 1.0 mM of ethylene glycol-bis[β-aminoethyl ether], 10 μg/mL of leupeptin, and 10 μg/mL of pepstatin A). Cells were then scraped from the walls of flasks, homogenized with a Branson Sonifier cell disrupter, and centrifuged on a Sorvall centrifuge at 13,000 rpm at 4°C for 20 minutes. The pellets were resuspended in homogenized buffer at 800 μg/mL and stored at −80°C, if not used immediately. Both competitive and saturation binding assays were performed in 96-well microtiter plates, using the Millipore MultiScreen System (Bedford, MA). For the competitive binding assay, 40 μg of the membrane protein was incubated with 0.05 nM of ^{64}Cu-DOTA-cetuximab at room temperature for 2 hours in a total volume of 250 μL of binding buffer (0.1% bovine serum albumin [BSA] in phosphate-buffered saline [PBS]) in the presence or absence of 0.1–60 nM of unlabeled cetuximab. After the incubation, the reaction buffer was removed by using a vacuum drain and the cells were washed two times with binding buffer. The plates were counted on the microbeta counter after loading 25 μL of scintillation cocktail into each well. The radioactivity bound to cells was plotted versus the increasing concentration of cetuximab to determine the best-fit IC_{50} values by using Prism software (v. 4.0; GraphPad, San Diego, CA). For saturation binding experiments, ^{64}Cu-DOTA-cetuximab (0.05–32 nM) was incubated with 40 μg of A431 membrane protein for 2 hours at room temperature, followed by the same procedure for competitive binding, as described above. Nonspecific binding was determined by conducting the assay in the presence of an excess (200 nM) unlabeled cetuximab. Specific binding was obtained by the subtraction of nonspecific binding from total binding. The dissociation constant (K_D) and receptor density (B_{max}) were estimated from the nonlinear fitting of the specific binding versus the concentration of ^{64}Cu-DOTA-cetuximab, using Prism software. For statistical considerations, two separate experiments for both competitive and saturation binding assays were performed in triplicate.

In Vivo Biodistribution and Micro-PET Imaging Studies

Animal studies were conducted in accordance with the highest standards of care, as outlined in the National Institutes of Health's (NIH; Bethesda, MD) *Guide for Care and Use of Laboratory Animals* and the policy and procedures for animal research at the Washington University School of Medicine. The biodistribution and uptake of ^{64}Cu-DOTA-cetuximab were determined in the A431 and MDA-MB-435 tumor-bearing nude mice. Following injection of the mice with aliquots of ^{64}Cu-DOTA-cetuximab (100 μL, 0.6 MBq, 1.2 μg) through the tail vein, blood, organs, and tumors were removed from animals euthanized by cervical dislocation at 4, 24, and 48 hours postinjection ($n = 5$ for each group). The 5 mice that were sacrificed at 48 hours postinjection were housed in individual metabolism cages for the collection of urine and feces at 4, 24, and 48 hours for the determination of the percent injected dose (%ID) excreted. For blocking studies, an excess of unlabeled cetuximab (1 mg) was injected into each mouse 20 hours before the radiolabeled mAb solution. The radioactivity of tissue samples was measured in a gamma counter. The percent injected dose per gram (% ID/g) and percent injected dose per organ (% ID/organ) were calculated by comparison with standards representing the injected dose per animal.

To delineate the uptake of ^{64}Cu-DOTA-cetuximab in A431 tumors, a group of 6 A431 tumor-bearing mice were anesthetized by the inhalation of 2% isofluorane and administrated with ^{64}Cu-DOTA-cetuximab. Three (3) mice were injected with an excess of unlabeled cetuximab (1 mg in 100 μL PBS per mouse) 20 hours prior to the administration of the imaging dose (5.6 MBq, 6 μg). Two (2) mice (control vs. block) were scanned for 10–30 minutes side by side at 4, 20, 27, and 46 hours after the administration of ^{64}Cu-DOTA-cetuximab on a micro-PET Focus (model 120 or 220; Concorde Microsystems, Knoxville, TN). In addition, the EGFR-mediated tumor uptake was also evaluated by the comparison of A431 tumors with MDA-MB-435 tumors by micro-PET. Four

(4) mice (2 mice for each tumor model) were injected with ^{64}Cu-DOTA-cetuximab (5.6 MBq, 6 μg), and two groups of 2 mice (A431 vs. MDA-MB-435 tumor mice) were imaged following the same protocol as described above. In a separate experiment, 4 mice bearing both EGFR-positive A431 and EGFR-negative MDA-MB-435 tumors on their contralateral mammary fat pads were injected with ^{64}Cu-DOTA-cetuximab (7.8 MBq, 20 μg) and scanned at 4 and 24 hours postinjection. High-resolution, coregistration micro-CT imaging was performed to monitor tumor volume and morphology at 24 hours postinjection. All micro-PET images were reconstructed, and regional tracer concentrations were quantified by the use of the ASIPRO software package (Concorde Microsystems). Quantitative data, such as accumulated activity of ^{64}Cu in tumor, kidney, and liver, were expressed as standardized uptake values (SUVs), which is defined as the counts per second per pixel in a region-of-interest (ROI) encompassing the entire organ divided by the total counts per second per pixel in the mouse.

In Vivo Metabolism in A431 Tumor-Bearing Nude Mice

Six (6) female nu/nu mice bearing 12-days A431 tumors were intravenously (i.v.) injected with 29.6–35.2 MBq (90 μg) of ^{64}Cu-DOTA-cetuximab. Blood, liver, and tumor were removed from the mice at 4 and 20 hours postinjection; the liver and tumor were rinsed with saline to remove as much blood as possible. The blood, liver, and tumor were homogenized in 0.1 M of ammonium citrate buffer (pH 7.4), using a Tekmar tissue homogenizer, and sonicated for 1 minute. The samples were purified by centrifugation (23,500 g, 30 minutes), and the supernatants were saved for size-exclusion HPLC analysis. Organ blanks, where ^{64}Cu-DOTA-cetuximab was added to tissues *ex vivo*, were performed to determine whether the extraction procedure affected the integrity of the radiolabeled antibody. For all metabolism and organ blank samples, a 0.1-mL sample was first passed through a 0.45-micron low-protein binding filter and then analyzed by size-exclusion HPLC on a Superose 12 HR 10/300 gel filtration column eluted with 20 mM of HEPES and 150 mM of NaCl (pH 7.4) buffer at a flow rate of 0.5 mL/min. Fractions were collected every minute and counted on a gamma counter.

Additional blood and organ samples were analyzed to determine the extraction efficiency. After homogenization and centrifugation, the supernatant was separated from the pellet and both were counted in a gamma counter. The extraction efficiency was measured as the counts from the supernatant divided by the total number of counts for pellet and supernatant. Results are expressed as the percentages of the total dose.

Statistical Comparisons

Data are expressed as the mean $\pm$ standard deviation. The Student's *t*-test (two-tailed) was performed with Prism software to determine the statistical significance at the 95% confidence level, with $p < 0.05$ being considered significantly different.

RESULTS

Radiochemistry and *In Vitro* Binding Affinity

It was determined that 5.5 DOTA chelators were attached per molecule of cetuximab, resulting in a specific activity of ^{64}Cu-DOTA-cetuximab, ranging from 0.4 to 1.1 MBq/μg. The variance in this specific activity was typically a result of the specific activity of the ^{64}Cu produced. The radiolabeled conjugate was purified by using either a Bio-spin 6 column filter or size-exclusion HPLC and was confirmed to be greater than 95% radiochemical purity by size-exclusion HPLC.

The binding affinity of ^{64}Cu-DOTA-cetuximab was determined by competitive displacement, using increasing concentrations of unlabeled cetuximab in highly EGFR-expressing A431 and low-expressing MDA-MB-435. The capacity of ^{64}Cu-DOTA-cetuximab to inhibit EGFR, presented as IC_{50} to EGFR-expressing carcinoma A431 cells, was determined to be 3.41 nM (95% confidence intervals [CIs] of 2.83–4.11 nM); however, there was no binding observed in EGFR-negative MDA-MB-435 cells (Fig. 1A). Nonspecific binding was tested in both cell lines by the addition of 50 nM of unlabeled cetuximab before the addition of ^{64}Cu-DOTA-cetuximab. Incubation of ^{64}Cu-DOTA-cetuximab with A431 cells in the presence of 50 nM of unlabeled cetuximab inhibited the binding by more than 90%, suggesting $<$10% nonspecific binding. In MDA-MB-435 cells, less than 10% of ^{64}Cu-DOTA-cetuximab bound was observed at all concentrations

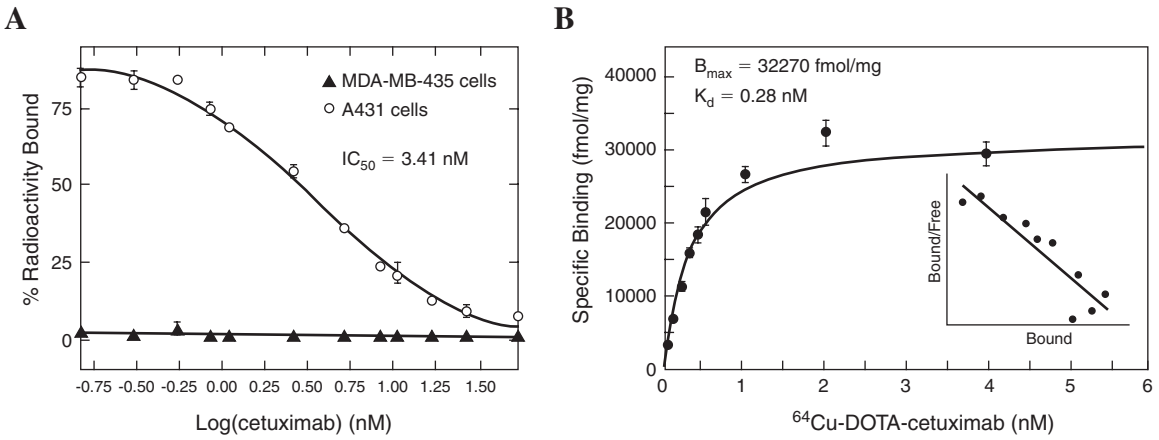

Figure 1. **(A)** Competitive binding curves of cetuximab versus ^{64}Cu-DOTA-cetuximab in A431 (epidermal growth-factor receptor [EGFR]-positive) and MDA-MB-435 (EGFR-negative) cells. IC_{50} of ^{64}Cu-DOTA-cetuximab to A431 is 3.410 nM (95% confidence intervals [CIs]: 2.832–4.107 nM). Each data point represents the mean ± standard error of the mean (SEM) of triplicate measurements. **(B)** Saturation binding curves of ^{64}Cu-DOTA-cetuximab to A431 cells. The K_D of ^{64}Cu-DOTA-cetuximab was determined to be 0.28 nM (95% CIs: 0.20–0.37 nM) and the EGFR concentration in A431 cells (B_{max}) was 32,270 fmol/mg (95% CIs: 29,746–34,795 fmol/mg). Each data point represents the mean ± SEM of triplicate measurements.

of unlabeled cetuximab with no dose dependence, demonstrating that the uptake of ^{64}Cu-DOTA-cetuximab was only nonspecific in this cell line.

The binding affinity of ^{64}Cu-DOTA-cetuximab was also investigated by determining the equilibrium dissociation constant (K_D) and the maximum specific binding (B_{max}) of radiolabeled conjugate to A431 cells in a saturation binding assay. In a control experiment, a large excess of unlabeled cetuximab was added to cells to saturate the EGFR in order to demonstrate binding specificity. A representative saturation binding curve and Scatchard transformation of ^{64}Cu-DOTA-cetuximab to A431 cells are shown in Figure 1B. The data show that ^{64}Cu-DOTA-cetuximab bound to a single class of binding sites with a K_D of 0.28 nM (95% CIs of 0.20–0.37 nM) and a maximum binding capacity of 32,270 fmol/mg of protein (95% CIs of 29,746–34794 fmol/mg). The obtained K_D and B_{max} values are

Table 1. Tissue Distribution of ^{64}Cu-DOTA-Cetuximab in A431 and MDA-MB-435 Tumor Bearing Mice

	A431				*MDA-MB-435*
Tissue	*4 hours* (n = *8)*	*24 hours* (n = *17)*	*24 hours bl* (n = *9)*	*48 hours* (n = *13)*	*24 hours* (n = *5)*
Blood	30.05 ± 6.09	16.47 ± 4.19	19.75 ± 5.99	12.56 ± 3.35	13.67 ± 1.38
Lung	10.70 ± 2.10	6.83 ± 1.64	8.71 ± 2.74	6.29 ± 1.07	5.52 ± 0.70
Kidney	6.04 ± 0.94	4.25 ± 0.92	5.60 ± 1.62	5.05 ± 0.60	3.61 ± 0.39
Liver	17.60 ± 6.11	12.70 ± 4.88	11.07 ± 2.89	15.34 ± 2.94	9.55 ± 3.29
Spleen	6.05 ± 2.18	5.08 ± 2.47	6.94 ± 3.03	5.57 ± 1.87	3.46 ± 0.31
Heart	7.50 ± 1.98	4.68 ± 1.03	5.82 ± 2.28	3.98 ± 0.73	3.43 ± 0.27
Stomach	1.97 ± 0.39	1.68 ± 0.65	2.37 ± 0.80	2.12 ± 0.34	1.26 ± 0.46
Intestines	9.21 ± 4.19	6.97 ± 3.37	7.91 ± 2.49	9.14 ± 2.31	5.54 ± 0.49
Muscle	2.04 ± 1.08	2.22 ± 0.48	2.86 ± 0.86	1.87 ± 0.51	1.97 ± 0.16
Tumor	5.45 ± 1.94	18.49 ± 6.40	10.69 ± 2.72	22.92 ± 6.32	2.60 ± 0.35
Tumor : blood	0.19 ± 0.026	1.15 ± 0.091	0.56 ± 0.033	1.84 ± 0.080	0.32 ± 0.26
Tumor : muscle	2.96 ± 0.41	8.61 ± 0.84	3.81 ± 0.18	12.4 ± 0.52	2.32 ± 2.04

Data are presented as the percent injected dose per g ± standard deviation.

in agreement with the literature data for K_D of unlabeled cetuximab and binding sites of A431 cells, suggesting that the conjugation procedure of DOTA to cetuximab did not affect the binding affinity of the antibody to A431 cells.[7,20]

In Vivo Biodistribution and Micro-PET Imaging Studies

The biodistribution of ^{64}Cu-DOTA-cetuximab was performed in A431 and MDA-MB-435 tumor-bearing mice, and the tissue uptake is shown in Table 1 and Figure 2. The uptake of ^{64}Cu-DOTA-cetuximab in A431 tumors increased steadily from 4 to 48 hours after the administration of ^{64}Cu-DOTA-cetuximab (4 hours: 5.45% ± 1.94% ID/g; 48 hours: 22.92% ± 6.32% ID/g). The tumor uptake at 24 and 48 hours postinjection was significantly higher ($p < 0.03$) than the uptake at both time points in all other tissues, except for the blood at 24 hours. There was a slow blood clearance of ^{64}Cu-DOTA-cetuximab, with 30.05% ± 6.09% ID/g at 4 hours to 12.56% ± 3.35% ID/g remaining at 48 hours, which is a common feature of intact mAbs. EGFR-mediated uptake of ^{64}Cu-DOTA-cetuximab in A431 tumors was demonstrated by the injection of an excess of unlabeled cetuximab 20 hours prior to tracer injection and by comparison with low-EGFR-expressing MDA-MB-435 tumor xenografts. There was a significant difference in the EGFR-positive tumor uptake of ^{64}Cu-DOTA-cetuximab, compared to that of the blocked uptake at 24 hours (18.49% ± 6.40% vs. 10.69% ± 2.72% ID/g; $p < 0.002$). The negative control tumor, MDA-MB-435, showed a ^{64}Cu-DOTA-cetuximab uptake of 2.6% ± 0.35% ID/g at 24 hours, and this uptake value was significantly lower than the uptake value at the same time points for the A431 tumors ($p < 0.03$). All other tissues showed a similar uptake of ^{64}Cu-DOTA-cetuximab in A431 tumors with or without the administration of cetuximab, and MDA-MB-435 tumors at 24 hours postinjection.

The tumor:blood and tumor:muscle ratios increased from 4 to 48 hours postinjection. At 4 hours, the tumor:blood ratio was 0.19 ± 0.03, and this increased to 1.84 ± 0.08 at 48 hours. Even though the tumor uptake at 24 and 48 hours was not significantly different ($p = 0.07$), the tumor:blood ratio at 48 hours (1.84 ± 0.08) was higher than at 24 hours (1.15 ± 0.09) ($p < 0.001$). Tumor:muscle ratio increased from 2.96 ± 0.40 at 4 hours to 12.4 ± 0.50 at 48 hours postinjection. The tumor:liver and tumor:kidney ratios leveled out at 24 hours postinjection (1.65 ± 0.21 and 4.41 ± 0.35, respectively).

Kidney uptake in A431 tumor-bearing mice remained stable from 4 to 48 hours postinjection (6.04% ± 0.94% ID/g and 5.05% ± 0.60% ID/g). In addition, the radioactivity in the liver remained fairly constant, from 17.60% ± 6.11% ID/g at 4 hours to 15.34% ± 2.94% ID/g at 48 hours. The excretion data in A431 tumor-bearing mice demonstrated that only 0.97% ± 0.52% ID of ^{64}Cu was excreted from the urine by 4 hours postinjection. By 24 hours postinjection, ~18% ID of ^{64}Cu-DOTA-cetuximab activity was found in the urine and feces and ~34% ID of ^{64}Cu-DOTA-cetuximab activity in urine and feces at 48 hours postinjection (Table 2).

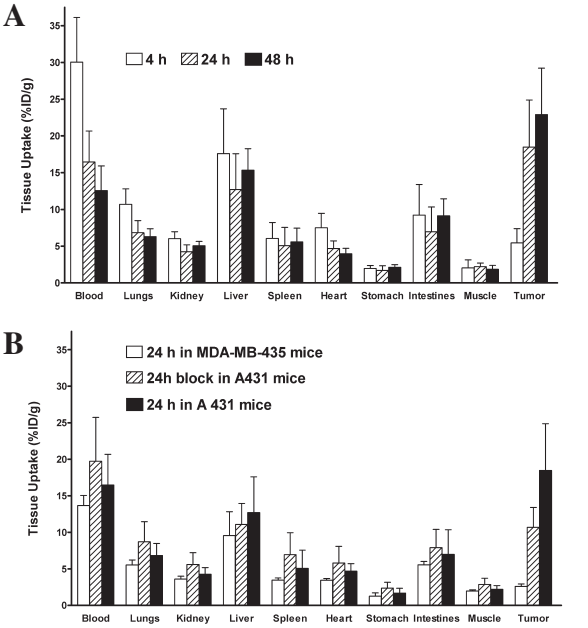

Figure 2. Biodistribution of ^{64}Cu-DOTA-cetuximab in epidermal growth-factor receptor (EGFR)-positive A431 and EGFR-negative MDA-MB-435 tumor-bearing nude mice. Data are presented as percent injected dose per gram ± standard deviation, $n = 5$ for each time point. Bl, blood; lg, lung; kd, kidney; lv, liver; sp, spleen; ht, heart; st, stomach; Int, intestines; mu, muscle; tu, tumor. **(A)** Tissue uptake of ^{64}Cu-DOTA-cetuximab in A431 tumor xenografts at 4 ($n = 8$), 24 ($n = 17$), and 48 hours ($n = 13$) postinjection. **(B)** Comparison of tissue uptake in A431 (control [$n = 17$] and block [$n = 9$] or MDA-MB-435 tumor xenografts ($n = 5$) at 24 hours postinjection. The group of 9 A431 tumor-bearing mice received 1 mg of unlabeled cetuximab per animal 20 hours prior to the administration of the radioactive dose.

Table 2. Excretion of ^{64}Cu-DOTA-Cetuximab in A431 Tumor-Bearing Mice

	^{64}Cu-DOTA-cetuximab		
	4 hours	*24 hours*	*48 hours*
Urine	0.97 ± 0.52	1.06 ± 0.65	1.87 ± 0.77
Feces	0.47 ± 0.14	15.48 ± 2.18	13.81 ± 1.83

All data are reported as the percent injected dose ± standard deviation.

Micro-PET imaging was performed at 19 or 20 hours and 46 or 48 hours after the injection of ^{64}Cu-DOTA-cetuximab in A431 and MDA-MB-435 tumor-bearing mice and in mice contralaterally bearing both A431 and MDA-MB-435 tumors. Tumor xenografts were clearly visible on the micro-PET images of all A431 tumor-bearing mice, which are shown in Figure 3. Also, as in the biodistribution studies, a significant reduction of tumor uptake was observed in A431 mice receiving a blocking dose of unlabeled cetuximab (1 mg, 20 hours in advance) (Fig. 3A). There was also a significantly lower uptake in MDA-MB-435 tumors, compared to A431 tumors (Fig. 3B). Coregistered micro-PET/computed tomography (CT) images were obtained at 24 hours postinjection for ^{64}Cu-DOTA-cetuximab in mice bearing both A431 and MDA-MB-435 tumors (Fig. 3). Consistent with the biodistribution data, there was a higher uptake in the A431 tumor than in the MDA-MB-435 tumor. The accumulation of radioactivity in livers was also visualized.

SUVs were also determined for tumors, livers, and kidneys (Fig. 4). Tumor uptake of ^{64}Cu-DOTA-cetuximab in A431 mice at all time points examined was greater than that in A431 mice administrated unlabeled cetuximab. A good agreement between the SUV analysis and the biodistribution analysis for the tumor uptake (Fig. 4A) was observed. The tumor uptake cleared slowly and represented nearly the same radioactivity by 46 hours postinjection. In addition, nonspecific liver uptake was observed in A431 tumor-bearing mice (Fig. 4B). Comparison of the uptake in tumor, liver, and kidneys by SUV between A431 tumor-bearing mice and MDA-MB-435 tumor-bearing mice is shown in Figure 4C. The data showed that there was a significantly greater uptake of ^{64}Cu-DOTA-cetuximab in A431 tumor than in MDA-MB-435 tumor at 24 hours ($p < 0.05$), and that the uptake in the liver or kidneys was significantly lower than the uptake in A431 tumors ($p < 0.02$).

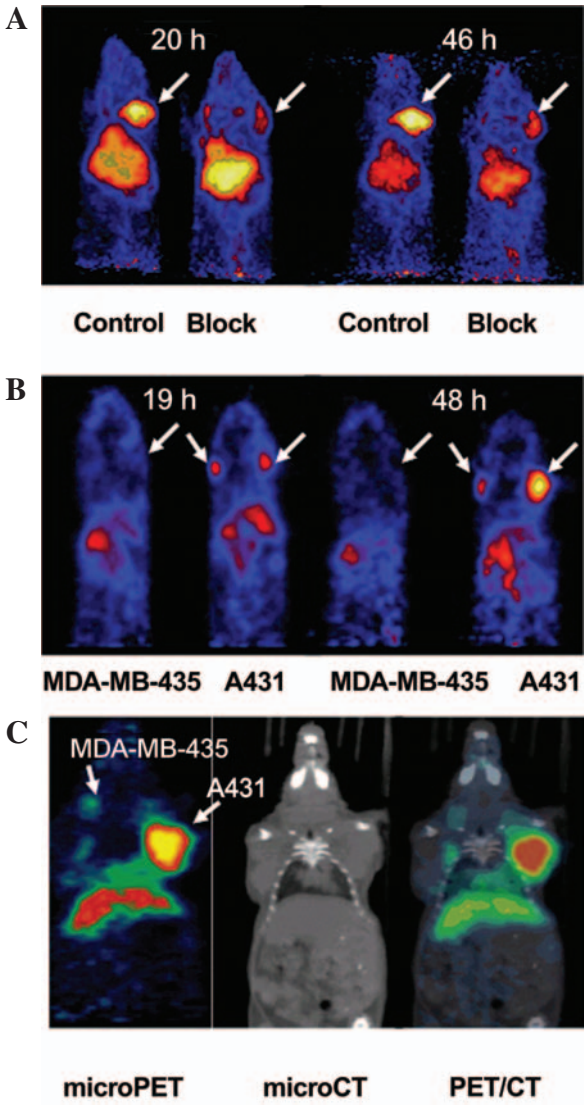

Figure 3. **(A)** Projection microPET images of A431 tumor-bearing nude mice after 20 and 46 hours postadministration of ^{64}Cu-DOTA-cetuximab, with and without an injected blocking dose 20 hours prior to the imaging dose (5.6 MBq, 6 μg, left; 5.6 MBq, 1 mg of cetuximab, right). Arrow points to tumor. **(B)** Coronal micro-PET images of ^{64}Cu-DOTA-cetuximab in A431 (epidermal growth-factor receptor [EGFR]-positive) and MDA-MB-435 (EGFR-negative) tumor-bearing mice after 19 and 48 hours postadministration of ^{64}Cu-DOTA-cetuximab. Arrow points to tumor. **(C)** Micro-PET/computed tomography coregistration images of ^{64}Cu-DOTA-cetuximab in a mouse bearing both A431 and MDA-MB-435 tumors (arrow) at 24 hours postinjection.

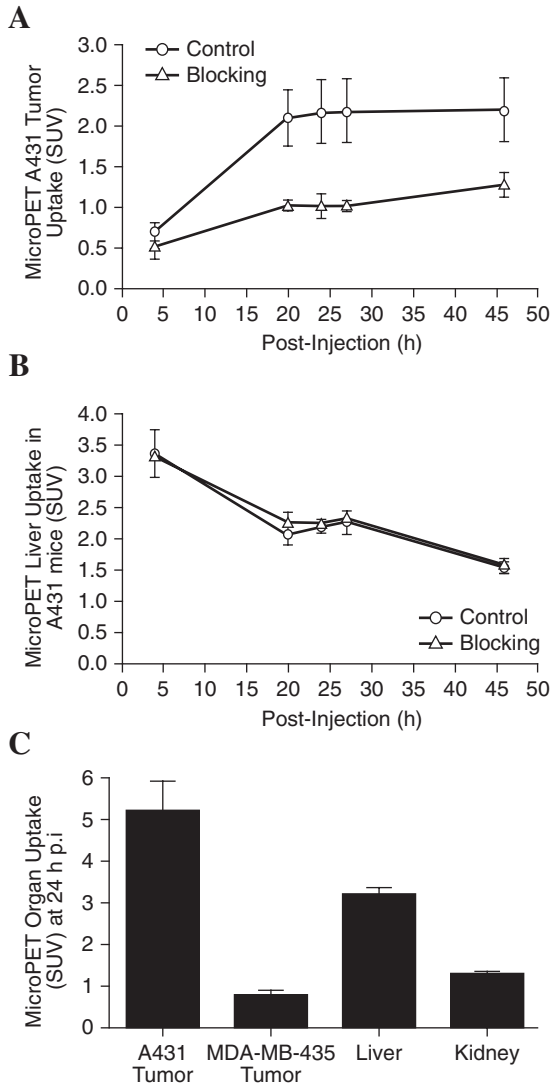

Figure 4. Standard uptake values (SUV) obtained from microPET images of ^{64}Cu-DOTA-cetuximab in tumor-bearing mice. **(A)** A431 tumor uptake of ^{64}Cu-DOTA-cetuximab with and without an injection of unlabeled cetuximab at various times of postinjection. **(B)** Liver uptake of ^{64}Cu-DOTA-cetuximab in A431 tumor-bearing mice with and without an injection of unlabeled cetuximab at various times of postinjection. **(C)** Organ uptake of ^{64}Cu-DOTA-cetuximab in mice bearing both A431 and MDA-MB-435 tumors at 24 hours postinjection.

In Vivo Metabolism in A431 Tumor-Bearing Nude Mice

By size-exclusion chromatography, ^{64}Cu-DOTA-cetuximab elutes at approximately 23 minutes, corresponding to a ~150-kDa protein (Fig. 5). Liver, tumor, and blood sample homogenates from A431 tumor-bearing mice were obtained at 4 and 20 hours postinjection of ^{64}Cu-DOTA-cetuximab and were analyzed by size-exclusion chromatography to determine the extent of ^{64}Cu transchelation to other proteins and catabolites. Representative size-exclusion chromatograms of liver extracts obtained from rats sacrificed at 4 hours postinjection revealed that ^{64}Cu-DOTA-cetuximab undergoes a transchelation of ^{64}Cu- to ^{64}Cu-labeled proteins eluting at 29 and 33 minutes, corresponding to ~31 and ~11 kDa proteins, respectively. Small-molecular-weight catabolites were also present, eluting at 36 minutes, corresponding to a molecular weight <5 kDa. The liver extracts at 20 hours postinjection revealed increased transchelation to the same protein masses.

Analysis of tumor extracts at 4 and 20 hours postinjection showed a greater degree of transchelation of ^{64}Cu and/or catabolism, with radioactivity peaks corresponding to molecular weight of ~11 and less than 5 kDa. In addition, a ^{64}Cu-labeled species eluted at 16 minutes, corresponding to a very large molecular weight (>1000 kDa), possibly indicating aggregated protein or mAbs.

The percentage of authentic intact (%AI) ^{64}Cu-DOTA-cetuximab antibody (see Table 3) was calculated for the blood, liver, and tumor homogenates at all time points. This calculation accounts for ^{64}Cu incorporation into other proteins, as determined by the integration of peaks from size-exclusion HPLC chromatograms and also corrects for protein-extraction efficiency.[21]

Organ blank experiments were carried out to ensure that the species observed after an i.v. injection of the radiolabeled complexes were, indeed, the result of *in vivo* processes versus the extracellular incorporation of ^{64}Cu into proteins

Table 3. Amount of Authentic Intact (AI) ^{64}Cu-DOTA-Cetuximab in A431 Tumor-Bearing Mice

	^{64}Cu-DOTA-cetuximab		
	0 hours	*4 hours*	*24 hours*
Blood	96.70	96.07 ± 2.91	96.15 ± 1.94
Liver	95.45	33.98 ± 12.95	32.75 ± 4.95
Tumor	86.10	15.65 ± 6.70	9.09 ± 4.69

Values at 4 h and 24 h are reported as %AI ± standard deviation. (n = 4), except for 4 hours blood, which is n = 3. Values at 0 hours are reported as %AI (n = 1).

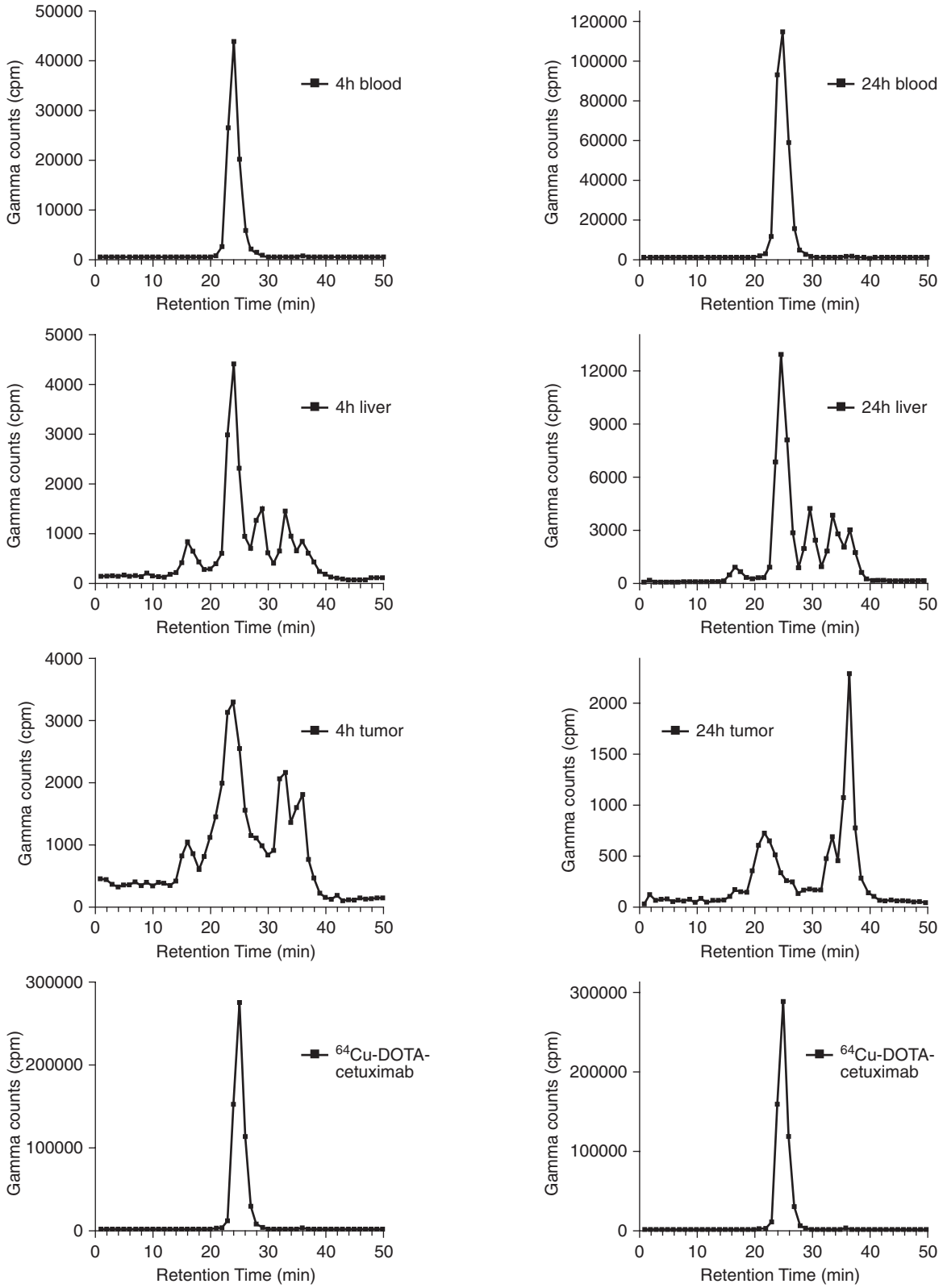

Figure 5. Size-exclusion high-performance liquid chromatography analyses of blood, liver, and tumor samples at 4 and 24 hours after an injection of ^{64}Cu-DOTA-cetuximab in A431 tumor-bearing mice.

released upon lysing the cells during homogenization and/or sonication. The ^{64}Cu-DOTA-cetuximab injectate was added *ex vivo* to liver and blood samples from noninjected mice, and the metabolism procedures were performed. These control experiments indicated that the observed incorporation of radiometal into intracellular proteins was most likely owing to metabolic processes *in vivo* and was not merely the result of the techniques used to extract the metabolites from the organs, except in the case of the tumor blank samples.

DISCUSSION

Cetuximab, an anti-EGFR mAb, has shown considerable activity in the treatment of metastatic colorectal cancer that is resistant to chemotherapy and also is under ongoing investigational studies for the treatment of non-small-cell lung cancer and pancreatic cancer. However, the lack of a predictive marker to predict responders to EGFR-targeted mAb therapy limits the use of this agent to patients with detectable EGFR expression.

There have been several recent reports in the literature on whether the response of cancer to cetuximab is correlated to the EGFR mRNA copy number or EGFR protein levels. No correlation has been found between the antitumor activity of cetuximab and the levels of EGFR expression in colorectal, lung, or pancreatic cancer.[22–24] Moroni et al. demonstrated a correlation in response to cetuximab in patients with metastatic colorectal cancer and EGFR copy number.[25] Vallbohmer et al. did not find a significant correlation between intratumoral EGFR gene expression and response, possibly because of a small sample size and low response rate.[26] However, they observed that patients with a higher gene expression of EGFR had a shorter overall survival. It has also been reported that even patients with no detectable EGFR by immunohistochemistry techniques have the potential to respond to cetuximab.[27] These conflicting reports reflect that, possibly, a more quantitative measure of EGFR is needed to assess EGFR status in patients in order to accurately determine whether there is any correlation between EGFR gene expression and/or EGFR protein levels and response to cetuximab. In addition, the use of a PET marker of cetuximab might assist in the dosing of cetuximab to assure that patients are receiving high enough doses to be effective.

Although there is evidence that the expression of EGFR does not necessarily correlate with the therapeutic efficacy of cetuximab therapy, having an imaging biomarker for EGFR expression may still be important. Imaging EGFR expression has been explored with the murine antibody, 225, labeled with ^{111}In and SPECT imaging,[28] whereas the chimeric antibody cetuximab has been labeled with ^{111}In[11,29,30] and ^{99m}Tc[31,32] for SPECT imaging. A recent report compared the uptake of the positron-emitting radionuclide, ^{89}Zr, radiolabeled to cetuximab with that of the ^{177}Lu- and ^{88}Y-labeled antibody.[10,11,32,33] In this study, we set out to determine if PET/CT imaging with ^{64}Cu-DOTA-cetuximab may be a more sensitive and accurate measure of EGFR, compared to traditional methods.

We first determined the binding affinity of ^{64}Cu-DOTA-cetuximab to EGFR receptors in a high-expressing tumor-cell line, A431. High binding affinity of ^{64}Cu-DOTA-cetuximab for EGFR in A431 tumor membranes (K_D = 0.28 nM) was determined, and Scatchard analysis confirmed a high EGFR concentration in the A431 tumors (32,270 fmol/mg protein). These data demonstrate that conjugating ^{64}Cu-DOTA to cetuximab does not adversely affect the binding of cetuximab to EGFR. To the best of our knowledge, these data represent the first quantitative binding affinity data for a radiolabeled cetuximab antibody with an EGFR-positive cell line. Wen et al. reported that a DTPA-PEG-cetuximab conjugate retained 66% of the binding affinity of unconjugated cetuximab but did not report binding constants or IC_{50} values.[11]

The tumor uptake of ^{64}Cu-DOTA-cetuximab increased between 4 and 24 hours and then remained stable out to 48 hours; however, the concentration of ^{64}Cu-DOTA-cetuximab in the blood decreased, thereby increasing the tumor to blood ratio at 48 hours. Blocking of ^{64}Cu-DOTA-cetuximab uptake with unlabeled cetuximab was observed at both 24 and 48 hours, as well as decreased tumor uptake in a low-EGFR-expressing tumor model (MDA-MB-435). These data demonstrate the specificity of ^{64}Cu-DOTA-cetuximab for the high-EGFR-expressing A431 tumor. Perk et al. reported the biodistribution of positron-emitting ^{89}Zr-deferrioxamine-cetuximab, and the uptake in the tumor, blood, and muscle are comparable to ^{64}Cu-DOTA-cetuximab.[33] The liver uptake of ^{89}Zr-labeled cetuximab at 24 hours was somewhat lower (~10% ID/g) than was observed for the ^{64}Cu-labeled

conjugate (17.6% ± 0.60% ID/g), although the ^{89}Zr uptake in the liver increased over time from ~10% to ~20% ID/g at 144 hours. Although both ^{89}Zr and ^{64}Cu have been shown to give high-quality PET images in clinical studies when radiolabeled to mAbs,[34,35] a disadvantage of ^{64}Cu is that the shorter half-life limits the imaging times to 48 hours, or possibly 72 hours postinjection, whereas the ^{89}Zr can be followed out to 144 hours. Comparison of ^{64}Cu-DOTA-cetuximab with ^{111}In-DTPA-PEG-cetuximab at 48 hours postinjection shows higher % ID/g blood uptake (12.56% vs. 1.4%) with improved tumor uptake (22% vs. 8.7%) and a markedly lower liver uptake (14.3% vs. 25.5%).

Cai et al. reported the biodistribution of ^{64}Cu-DOTA-cetuximab in seven different EGFR-expressing tumor-bearing mouse models.[13] The highest tumor uptake was reported for U87MG, which at 48 hours, showed approximately 12% ID/g. In this study, we report 23% ID/g for A431 tumors, which was not described in the Cai et al. study. Although the tumor uptake in our studies was higher, the tumor:blood and tumor:muscle ratios were comparable between A431 and U87MG tumor-bearing mice.

It has been established that DOTA is not the ideal chelator for ^{64}Cu, as ^{64}Cu-DOTA is not highly stable *in vivo* and ^{64}Cu dissociates and binds to proteins in the blood and liver.[36] Cross-bridged macrocycles show much greater stability with ^{64}Cu; unfortunately, the enhanced kinetic and *in vivo* stability for biomolecule conjugates, such as CB-TE2A-conjugated Tyr^3-octreotate, results in the need for harsher labeling conditions (95°C for 60 minutes),[37] which are incompatible for protein labeling. Surprisingly, a relatively high tumor uptake of ^{64}Cu-DOTA-cetuximab was observed at 48 hours postinjection (22.92% ± 6.32% ID/g), whereas the liver and blood uptake were significantly less (15.34% ± 2.94% and 12.56% ± 3.35% ID/g, respectively; $p < 0.01$).[33]

Metabolism experiments were performed to determine the extent of ^{64}Cu transchelation to blood, liver, and tumor proteins. These results showed there was very little metabolism of ^{64}Cu-DOTA-cetuximab in the blood out to 24 hours postinjection (>95% AI at all time points), confirming that the slow blood clearance was primarily owing to slow clearance of the intact antibody. There was relatively rapid metabolism in the liver (~30% AI at 4 hours); however, there was little further metabolism between 4 and 24 hours postinjection. Metabolism in the tumor was rapid, although the tumor uptake continued to increase out to 48 hours postinjection, suggesting that the metabolites do not rapidly clear from the tumor.

Liver metabolism studies demonstrated that the ^{64}Cu was shown to transchelate to three proteins, as shown by size-exclusion chromatography. Some of the protein-bound ^{64}Cu in the liver at 4 and 20 hours postinjection eluted in a peak corresponding to a molecular weight of 31 kDa, consistent with previous results showing SOD as a primary radiolabeled protein in rat liver.[36,38] Another radiolabeled protein, with an apparent molecular weight of ~11 kDa, was also observed in the size-exclusion chromatograms for both liver and tumor, consistent with the apparent molecular weight of metallothionein, a class of ubiquitous, low-molecular-weight, cysteine-rich, metal-binding proteins that function in the metabolism of zinc and copper. Previous studies performed in our lab have shown similar results, with sizes ranging from 11 to 14 kDa being attributed to metallothionein.[36]

The tumor extracts at 4 hours postinjection showed significant transchelation to a protein of size ~11 kDa as well as degradation to low-molecular-weight metabolites (<5 kDa). At 20 hours postinjection, even greater amounts of ^{64}Cu were bound to <5-kDa metabolites. Copper-64 activity was observed at a retention time corresponding to a protein weight of greater than 1000 kDa, and this is believed to be owing to protein aggregation or, possibly (although less likely), the ^{64}Cu-DOTA-cetuximab is bound to EGFR-containing protein complexes.[39] In addition, it is important to note that ^{64}Cu-labeled SOD was not observed in either time point in the tumor. One possible explanation could be that the amount of metallothionein present in the tumor is much greater than what is found in other tissues, such as the liver. Murphy et al. showed that hypoxic conditions in human A431 tumors caused significant increase in the levels of metallothionein IIA mRNA, which were also confirmed by Western blotting.[40] If there are high levels of metallothionein in these tumors, then the ^{64}Cu may preferentially transchelate to this over the potentially lower levels of SOD.

CONCLUSIONS

In summary, ^{64}Cu-DOTA-cetuximab was evaluated as a PET-imaging agent for EGFR-positive

tumors. High binding affinity of ^{64}Cu-DOTA-cetuximab for EGFR (0.28 nM) was demonstrated in A431 cell membranes, and specific uptake of the tracer was demonstrated in A431 tumor-bearing mice. The uptake of ^{64}Cu-DOTA-cetuximab increased over time, whereas the tracer cleared from the blood. The tumor was clearly visualized by micro-PET in A431 tumor-bearing mice. ^{64}Cu-DOTA-cetuximab is a potential tracer for imaging EGFR-positive tumors in humans. Although it is still not clear whether ^{64}Cu-DOTA-cetuximab may be an accurate predictor of response to cetuximab therapy, this agent will noninvasively demonstrate the presence of EGFR as one of the (potentially) multiple receptor types in the tumor and may also help with dosing in patients to assure that the EGFR receptors are saturated.

ACKNOWLEDGMENTS

This research was supported by National Cancer Institute (NCI) grant no. P50CA9405604 (D. Piwnica-Worms, PI). The production of ^{64}Cu at the Washington University School of Medicine was supported by NCI grant no. R24 CA86307. Small-animal imaging at the Washington University School of Medicine was supported by NIH grant no. 5 R24 CA83060. The authors gratefully acknowledge Susan Adams and Martin Eiblmaier for their technical assistance, Nicole Fettig and Lori Strong for their small-animal imaging assistance, and Jerrel Rutlin for his data analysis.

REFERENCES

1. Grunwald V, Hidalgo M. The epidermal growth factor receptor: A new target for anticancer therapy. *Curr Probl Cancer* 2002;26:109.
2. Laskin JJ, Sandler AB. Epidermal growth factor receptors: A promising target in solid tumors. *Cancer Treat Rev* 2004;30:1.
3. Wong S. Cetuximab: An epidermal growth factor receptor monocolonal antibody for the treatment of colorectal cancer. *Clin Ther* 2005;27:684.
4. Cunningham D, Humblet Y, Siena S, et al. Cetuximab monotherapy and cetuximab plus irinotecan in irinotecan-refractory metastatic colorectal cancer. *N Engl J Med* 2004;351:337.
5. Saltz LB, Meropol NJ, Loehrer PJ, et al. Phase II trial of cetuximab in patients with refractory colorectal cancer that expresses the epidermal growth factor receptor. *J Clin Oncol* 2004;22:1201.
6. Mendelsohn J. Epidermal growth factor receptor inhibition by a monocolonal antobody as anticancer therapy. *Clin Cancer Res* 1997;3:2703.
7. Fan Z, Masui H, Altas I, et al. Blockage of epidermal growth factor receptor function by bivalent and monovalent fragments of C225 anti-epidermal growth factor receptor monoclonal antiobodies. *Cancer Res* 1993;53:4322.
8. Dadparvar S, Krishna L, Miyamoto C, et al. Indium-111-labeled anti-EGFr-425 scintigraphy in the detection of malignant gliomas. *Cancer* 1994;73:884.
9. Vallis KA, Reilly RM, Chen P, et al. A phase I study of ^{99m}Tc-hR3 (DiaCIM), a humanized immunoconjugate directed towards the epidermal growth factor receptor. *Nucl Med Commun* 2002;23:1155.
10. Goldenberg A, Masui H, Divgi C, et al. Imaging of human tumor xenografts with an indium-111-labeled anti-epidermal growth factor receptor monoconal antibody. *J Natl Cancer Inst* 1989;82:1616.
11. Wen X, Wu QP, Ke S, et al. Conjugation with (111)In-DTPA-poly(ethylene glycol) improves imaging of anti-EGF receptor antibody C225. *J Nucl Med* 2001;42:1530.
12. Nordberg E, Friedman M, Gostring L, et al. Cellular studies of binding, internalization and retention of a radiolabeled EGFR-binding affibody molecule. *Nucl Med Biol* 2007;34:609.
13. Cai W, Chen K, He L, et al. Quantitative PET of EGFR expression in xenograft-bearing mice using (64)Cu-labeled cetuximab, a chimeric anti-EGFR monoclonal antibody. *Eur J Nucl Med Mol Imaging* 2007;34:850.
14. McCarthy DW, Shefer RE, Klinkowstein RE, et al. The efficient production of high specific activity Cu-64 using a biomedical cyclotron. *Nucl Med Bio* 1997;24:35.
15. Rogers BE, Anderson CJ, Connett JM, et al. Comparison of four bifunctional chelates for radiolabeling monoclonal antibodies with copper radioisotopes: Biodistribution and metabolism. *Bioconjug Chem* 1996;7:511.
16. Sun X, Rossin R, Turner JL, et al. An assessment of the effects of shell cross-linked nanoparticle size, core composition, and surface PEGylation on *in vivo* biodistribution. *Biomacromolecules* 2005;6:2541.
17. Price JE, Polyzos A, Zhang RD, et al. Tumorigenicity and metastasis of human breast carcinoma cell lines in nude mice. *Cancer Res* 1990;50:717.
18. Velikyan I, Sundberg AL, Lindhe Ö, et al. Preparation and evaluation of ^{68}Ga-DOTA-hEGF for visualization of EGFR expression in malignant tumors. *J Nucl Med* 2005;46:1881.
19. Anderson CJ, Pajeau TS, Edwards WB, et al. *In vitro* and *in vivo* evaluation of copper-64-labeled octreotide conjugates. *J Nucl Med* 1995;36:2315.
20. Sato JD, Kawamoto T, Le AD, et al. Biological effects *in vitro* of monoclonal antibodies to human epidermal growth factor receptors. *Mol Biol Med* 1983;1:511.
21. Bass LA, Lanahan MV, Duncan JR, et al. Identification of the Soluble *in vivo* metabolites of Indium-111-diethylenetriaminepentaacetic acid-D-Phe^1-octreotide. *Bioconjug Chem* 1998;9:192.

22. Buchsbaum DJ, Bonner JA, Grizzle WE, et al. Treatment of pancreatic cancer xenografts with Erbitux (IMC-C225) anti-EGFR antibody, gemcitabine, and radiation. *Int J Radiat Oncol* 2002;54:1180.
23. Mukohara T, Engelman JA, Hanna NH, et al. Differential effects of gefitinib and cetuximab on non-small-cell lung cancer bearing epidermal growth factor receptor mutations. *J Natl Cancer Inst* 2005;97:1185.
24. Wild R, Fager K, Flefleh C, et al. Cetuximab preclinical antitumor activity (monotherapy and combination based) is not predicted by relative total or activated epidermal growth factor receptor tumor expression levels. *Mol Cancer Ther* 2006;5:104.
25. Moroni M, Veronese S, Benvenuti S, et al. Gene copy number for epidermal growth factor receptor (EGFR) and clinical response to anti-EGFR treatment in colorectal cancer: a cohort study. *Lancet Oncol* 2005;6: 279.
26. Vallbohmer D, Zhang W, Gordon M, et al. Molecular determinants of cetuximab efficacy. *J Clin Oncol* 2005; 23:3536.
27. Chung KY, Shia J, Kemeny NE, et al. Cetuximab shows activity in colorectal cancer patients with tumors that do not express the epidermal growth factor receptor by immunohistochemistry. *J Clin Oncol* 2005;23:1803.
28. Divgi C, Welt S, Kris FX, et al. Phase I and imaging trial of indium 111-labeled anti-epidermal growth factor receptor monoclonal antibody 225 in patients with squamous cell lung carcinoma. *J Natl Cancer Inst* 1991; 83:97.
29. Ke S, Wen X, Wu QP, et al. Imaging taxane-induced tumor apoptosis using PEGylated, ^{111}In-labeled annexin V. *J Nucl Med* 2004;45:108.
30. Wen X, Wu QP, Lu Y, et al. Poly(ethylene glycol)-conjugated anti-EGF receptor antibody C225 with radiometal chelator attached to the termini of polymer chains. *Bioconjug Chem* 2001;12:545.
31. Schechter NR, Yang DJ, Azhdarinia A, et al. Assessment of epidermal growth factor receptor with ^{99m}Tc-ethylenedicysteine-C225 monoclonal antibody. *Anticancer Drugs* 2003;14:49.
32. Schechter NR, Wendt RE, 3rd, Yang DJ, et al. Radiation dosimetry of ^{99m}Tc-labeled C225 in patients with squamous cell carcinoma of the head and neck. *J Nucl Med* 2004;45:1683.
33. Perk LR, Visser GW, Vosjan MJ, et al. (89)Zr as a PET surrogate radioisotope for scouting biodistribution of the therapeutic radiometals (90)Y and (177)Lu in tumor-bearing nude mice after coupling to the internalizing antibody cetuximab. *J Nucl Med* 2005;46:1898.
34. Perk LR, Visser OJ, Stigter-van Walsum M, et al. Preparation and evaluation of (89)Zr-Zevalin for monitoring of (90)Y-Zevalin biodistribution with positron emission tomography. *Eur J Nucl Med Mol Imaging* 2006;33: 1337.
35. Philpott GW, Dehdashti F, Schwarz SW, et al. RadioimmunoPET (MAb-PET) with Cu-64-labeled monoclonal antibody (MAb 1A3) fragments [F(ab′)2] in patients with colorectal cancers. *J Nucl Med* 1995;36:9P.
36. Boswell CA, Sun X, Niu W, et al. Comparative *in vivo* stability of copper-64-labeled cross-bridged and conventional tetraazamacrocyclic complexes. *J Med Chem* 2004;47:1465.
37. Sprague JE, Peng Y, Sun X, et al. Preparation and biological evaluation of copper-64-Tyr^3-octreotate using a cross-bridged macrocyclic chelator. *Clin Cancer Res* 2004;10:8674.
38. Bass LA, Wang M, Welch MJ, et al. *In vivo* transchelation of copper-64 from TETA-octreotide to superoxide dismutase in rat liver. *Bioconjug Chem* 2000;11:527.
39. Li S, Schmitz KR, Jeffrey PD, et al. Structural basis for inhibition of the epidermal growth factor receptor by cetuximab. *Cancer Cell* 2005;7:301.
40. Hill PA, Murphy G, Docherty AJ, et al. The effect of selective inhibitors of matrix metalloproteinases (MMPs) on bone resorption and the identification of MMPs and TIMP-1 in isolated osteoclasts. *J Cell Sci* 1994;107:3055.